Prell, W.L., Wang, P., Blum, P., Rea, D.K., and Clemens, S.C. (Eds.)
Proceedings of the Ocean Drilling Program, Scientific Results Volume 184

18. Data Report: Marine and Terrigenous Lipids in the Sediments from the South China Sea, Site 1148, Leg 184[1]

Ping'an Peng,[2] Chiling Yu,[2] Guodong Jia,[2] Jianfang Hu,[2]
Jianzhong Song,[2] and Gan Zhang[2]

ABSTRACT

Lipid compositions of sediments recovered during Ocean Drilling Program Leg 184 in the South China Sea have been identified and quantified. The identified lipids can be ascribed to terrigenous and marine sources. Terrigenous lipids are mainly C_{27}, C_{29}, C_{31} *n*-alkanes, C_{26}, C_{28}, C_{30} *n*-fatty acids, and *n*-alcohols, which were derived from leaf waxes of higher land plants and transported to the sea by airborne dust or fresh water. Marine lipids, mainly C_{37} and C_{38} alkenones, C_{30} diol, and C_{30} and C_{32} keto-ols, were from microalgae, notably haptophytes and eustigmatophytes. Elevated concentrations and accumulation rates of both terrigenous and marine lipids in the interval 202–245 meters composite depth (mcd) and 0–166 mcd were postulated to be related to the development of the East Asian monsoon at 6–8 Ma and enhanced variations of the developed East Asian monsoon after 3.2 Ma, respectively. The pronounced late Oligocene input of terrigenous lipids reflects the paleoenvironment of a newly opened, narrow basin, with restricted ocean waters and the proximity of continental runoff.

INTRODUCTION

The shipboard scientific party of Leg 184 sought to better understand the history and variability of the Asian monsoon system, which is a ma-

[1]Peng, P., Yu, C., Jia, G., Hu, J., Song, J., and Zhang, G., 2004. Data report: Marine and terrigenous lipids in the sediments from the South China Sea, Site 1148, Leg 184. *In* Prell, W.L., Wang, P., Blum, P., Rea, D.K., and Clemens, S.C. (Eds.), *Proc. ODP, Sci. Results,* 184, 1–16 [Online]. Available from World Wide Web: <http://www-odp.tamu.edu/publications/184_SR/VOLUME/CHAPTERS/209.PDF>. [Cited YYYY-MM-DD]
[2]State Key Laboratory of Organic Geochemistry, Guangzhou Institute of Geochemistry, Chinese Academy of Sciences, Wushan, Guangzhou 510640, People's Republic of China.
Correspondence author: **jiagd@gig.ac.cn**

Initial receipt: 3 September 2001
Acceptance: 15 December 2003
Web publication: 13 April 2004
Ms 184SR-209

jor component of the regional climate of Asia as well as global climate. Evolution of monsoonal climates in southern Asia is linked to the growth of the Himalayan-Tibetan orogeny (see papers and references in Ruddiman, 1997), the opening and closing of marginal seas (Wang et al., 1999), and changes in global climate, including atmospheric CO_2 levels (see papers and references in Ruddiman, 1997). The South China Sea (SCS) experiences both summer and winter monsoons, and its sediments record the erosion and weathering of surrounding rocks by tectonic orogens as well as the changes in global and regional climate. Parts of the major scientific objectives of Leg 184 are to obtain continuous sequences of hemipelagic sediments that record the East Asian climate history during the late Cenozoic, establish records of monsoonal proxies for the SCS, and establish stratigraphy ties between the SCS marine records and terrestrial records of China. It should thus be possible to accomplish the objectives by examining specific assemblages of terrigenous and marine components. Lipid biomarker compositions, which provide information on different types of terrigenous lipid sources and a detailed view of marine plankton groups contributing to the sedimentary organic matter, can play an important role in concerned studies.

For these purposes, a detailed molecular organic geochemical study was performed on downhole samples from Ocean Drilling Program (ODP) Sites 1147 and 1148 in the northern SCS, where we recovered a 861-m-long composite section spanning the last 30 m.y. Compilation of this data could elucidate the origin of sedimentary organic matter and determine various proxy signals of paleoenvironmental parameters. In addition, identifying and quantifying the major biomarkers for Sites 1147 and 1148 will add to the inventory of data for further molecular stratigraphic studies.

MATERIALS AND METHODS

Samples

The samples investigated were taken from Sites 1147 and 1148, mostly at an interval of 1.5 m for every core, and kept frozen until analysis. Site 1147 (18°50.11′N, 116°33.28′E; 3246 m water depth) was proposed to recover the continuous sequence of the uppermost hemipelagic sediments thought to be lost to slumping or channeling at Site 1148 (18°50.17′N, 116°33.94′E; 3294 m water depth). A total of 326 samples, covering a length of near 600 m, were analyzed.

Extraction of Soluble Organic Matter

About 3 g of each frozen sediment sample was placed into a 10-mL polytetrafluoroethylene centrifuge tube and thawed at room temperature. The samples were serially extracted with a rotary blender, using two 7-mL aliquots of methanol (MeOH), one 7-mL aliquot of trichloromethane (TCM):MeOH (1:1, v/v), and two 7-mL aliquots of TCM, each for 8 hr. The compounds $C_{24}D_{50}$ and $C_{16}D_{31}O_2H$ were added after the methanol extraction as standards for quantification. For each sample, the extracts were combined and back extracted by the addition of 15 mL of KCl solution. Then the separated water solution was extracted twice with 15 mL of TCM. The combined organic phase was concen-

trated to ~20 mL with a rotary evaporator at 35°C, dried with anhydrous Na_2SO_4, and concentrated again to ~0.5 mL.

Instrumental Analyses

Prior to instrumental analysis, the extracts were derivatized with bistrimethylsilyl-trifluoroacetamide in pyridine at ~20°C for 2 days. Gas chromatography (GC)–mass spectrometry was performed on a Finnigan GC8000-Voyager equipped with an on-column injector and fitted with a Chrompack fused silica capillary column (32 m × 0.30 mm). Helium was used as the carrier gas, and the oven was programmed from 45°C to 120°C at 10°C/min, followed by 4°C/min to 300°C (30 min hold time). The mass spectrometer was operated with an electron energy of 70 eV and an ion source temperature of 250°C and scanned over mass range *m/z* 50–700 with a cycle time of 1.0 s. Compound identifications are based on comparison of relative GC retention times and mass spectra with those in literature. Quantification of lipids was performed by integration of their peak areas and comparing with the internal standards in total ion chromatograms. The recovery of internal standards of *n*-alkane, fatty acid, and cholesterol added to the blank is 95.8%, 92.3%, and 99.7%, respectively, and that to the matrix (marine sediment Soxhlet extracted with benzene:MeOH [7:3, v:v] for 72 hr) is 94.8%, 90.8%, and 98.8%, respectively.

RESULTS AND DISCUSSION

Figure F1 shows the chromatograms of total lipid fractions (Sample 184-1148A-8H-2, 56–57 cm; 59.86 meters below seafloor). The compounds mainly consist of *n*-alkanes, fatty acids, alcohols, long-chain alkenones, diols, and keto-ols. Several of these compounds from both terrestrial plants and marine sources will be discussed according to compound classes.

F1. TIC and IC of *n*-alkanes, *n*-fatty acids, and *n*-alcohols, p. 9.

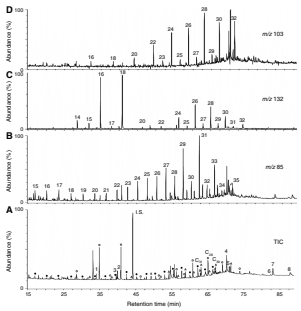

Terrigenous Lipids

Long-Chain *n*-Alkanes

n-Alkanes in the studied downhole sediments range in carbon number from 15 to 35; C_{25}–C_{33} *n*-alkanes are the most dominant homologues (Fig. F1B). An odd-over-even carbon number predominance, indicated from average carbon preference index (CPI) $CPI_{24–34}$ = 2.6 (ranging between 0.3 and 18.5) and odd-even predominance (OEP) = 3.3 (ranging between 0.1 and 12.4), was observed in nearly all samples, indicating a predominantly terrigenous origin of the long-chain *n*-alkanes (Fig. F2). These distributions resemble those of *n*-alkanes from leaf waxes of higher plants (Kolattukudy, 1976; Eglinton and Hamilton, 1967) and in eolian dust samples (Gagosian et al., 1981, 1987; Simoneit et al., 1977), supporting a terrigenous origin.

F2. CPI, OEP, and average chain length of *n*-alkanes, p. 10.

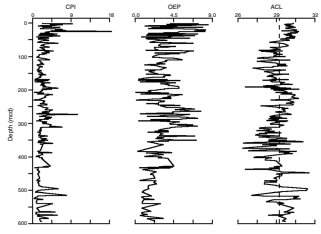

The average chain length changes from 26.4 to 31.6 (average = 29.2) (Fig. F2). It has been suggested that longer-chain compounds are produced by plants in warmer climates (e.g., Poynter et al., 1989) or are derived from grasslands, which may have, on average, longer chain lengths than leaf lipids from plants in rainforests (Cranwell et al., 1973). The observed shift in our data set will be addressed in future research.

Long-Chain Fatty Acids and *n*-Alcohols

Fatty acids in the downhole sediments range in carbon number from C_{14} to C_{32} (Fig. F1C) and *n*-alcohols occur in the carbon number range of C_{16}–C_{32} (Fig. F1D). The downhole distributions of C_{22}–C_{32} fatty acid and *n*-alcohol concentrations are similar to that of long-chain *n*-alkanes. Even carbon numbered long-chain compounds dominate the distributions of both compound groups. The dominance of the long-chain compounds, together with the observed strong even-over-odd carbon number predominance (for fatty acid and *n*-alcohols, average $CPI_{22–30}$ = 9.7 and 13.1, respectively), indicates a terrigenous origin for fatty acids and *n*-alcohols. Series of long-chain *n*-fatty acids and *n*-alcohols with a strong even carbon number predominance are characteristic constituents of surface waxes of higher plants (Kolattukudy, 1976). Therefore, the biological source of these compounds is closely related to that of the leaf wax–derived *n*-alkanes. An algal origin of the long-chain fatty acids, however, cannot be completely excluded (Volkman et al., 1998). Marine microalgae are not a major source of long-chain *n*-alcohols but may contain minor amounts of these compounds (for a review, see Volkman et al., 1998). However, the strong covariance of the concentrations of long-chain fatty acids and *n*-alcohols with the concentrations of *n*-alkanes, together with their high CPI values, indicate allochthonous sources of fatty acids and *n*-alcohols. In other words, higher plant leaf waxes are the main source.

Sectional Variations of Terrigenous Lipids

Total concentrations of C_{27}, C_{29}, and C_{31} *n*-alkanes in sediments (average = 0.47 µg/g dry sediment) vary in a large range between 0 and 12.33 µg/g dry sediment (Table T1). Three sections have relatively high values. They are the sections below 495 meters composite depth (mcd), 202–245 mcd, and 0–166 mcd. The highest values occur in the section between 202 and 245 mcd (Fig. F3). The accumulation rate variation pattern of *n*-alkanes shows the feature more pronouncedly (Fig. F4). Sectional variations of total long-chain *n*-fatty acids and *n*-alcohols are quite similar to those of *n*-alkanes (Figs. F3, F4).

The downhole variations of leaf wax components possibly result from changes in the different oceanographic and climatic settings, which determined the inputs of terrigenous lipids to Sites 1147 and 1148. The section below 495 mcd was deposited with a significant supply of terrigenous fine-grained clasts in the late Oligocene, which is the SCS-floor spreading phase (Briais et al., 1993). At that time, the newly opened, narrow basin, with restricted ocean waters and the proximity of continental runoff, led to an increase in terrigenous input. The much higher concentrations of terrigenous lipids in the section between 202 and 244 mcd, deposited at ~6–8 Ma when the eolian component of the loess red-clay sequence first appeared at the Chinese Loess Plateau (Ding et al., 1998), may be related to the development of the East Asian monsoon. And the section above 166 mcd with high, fluctuating concentrations of terrigenous lipids may indicate the enhanced variations of the developed monsoon since ~3.2 Ma.

T1. Concentrations of marine and terrigenous lipids, Sites 1147 and 1148, p. 16.

F3. Concentrations of *n*-alkane, *n*-alcohol, and *n*-fatty acid, p. 11.

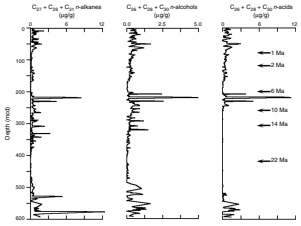

F4. Accumulation rates of *n*-alkane, *n*-alcohol, and *n*-fatty acid, p. 12.

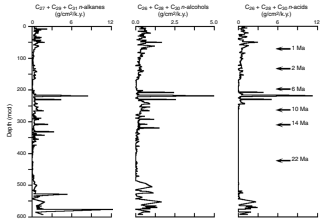

Marine Lipids

Long-Chain Alkenones

Sediment samples above 305.37 mcd contain C_{37} and C_{38} di- and triunsaturated methyl and ethyl ketones. High concentrations of these compounds were found in samples at the top of interval 0.56–61.76 mcd. Concentrations of those compounds in sediments in the interval 61.76–162.08 mcd are much lower and are trace in the interval 164.07–186.87 mcd (Table T1; Fig. F5). Some samples in the interval 202.57–305.37 mcd contain only $C_{37:2}$ ketone, but its concentrations are even higher than those at the top of interval 0.56–61.76 mcd.

Long-chain alkenones are exclusively biosynthesized by haptophyte algae like *Emiliania huxleyi* and *Gephyrocapsa* spp. (Volkman et al., 1980, 1995; Marlowe et al., 1984) and were detected in numerous marine sediments (e.g., Brassell et al., 1986), including the SCS (Pelejero and Grimalt, 1997). The $U^{k'}_{37}$ index, the ratio of the diunsaturated to the sum of the di- and triunsaturated C_{37} alkenones, is extensively used in paleoceanography as a temperature proxy. In this work, downhole $U^{k'}_{37}$ values in the alkenone-containing interval 0–186.7 mcd show a decreasing trend upward, which may indicate a general cooling process since ~5 Ma. In addition, high $C_{37:2}$ alkenone concentrations with the absence of $C_{37:3}$ alkenone in the interval 202.57–305.37 mcd may suggest higher sea-surface temperature in the late Miocene than the following period. However, although it has been shown that the $U^{k'}_{37}$ index is well correlated to $\delta^{18}O$ signal for *Globigerinoides sacculifer* for the past 550 k.y., the indexes show little agreement in samples older than that age (Brassell et al., 1986). For Sites 1147 and 1148, only the top section to the depth of ~40 m approximately corresponds to the past 550 k.y.; therefore, the downhole shift of $U^{k'}_{37}$ and $U^{k'}_{37}$-based sea-surface temperature, using the equation of Pelejero and Grimalt (1997), is tentatively given here and not discussed further in this report (Fig. F6).

F5. Concentrations of alkenones, diols, and keto-ols, p. 13.

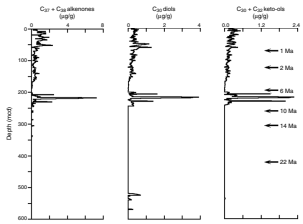

F6. $U^{k'}_{37}$ values and $U^{k'}_{37}$-based SST, p. 14.

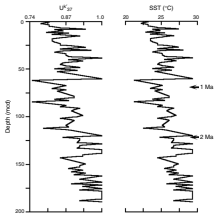

Alkyl Diols and Alkyl Keto-ols

Alkyl diols have been reported to occur in sediments from various areas (de Leeuw et al., 1981; see review in Versteegh et al., 1997). Their major sources are probably microalgae of the class Eustigmatophyceae (Volkman et al., 1992, 1999). Long-chain saturated C_{30} alkyl diols were detected in some samples, mainly above 244.77 mcd and below 519.35 mcd. Its downhole variation is similar to that of $C_{37:2}$ ketone (Table T1; Fig. F5).

C_{30} and C_{32} alkyl keto-ols are present in samples above 241.17 mcd. A deceasing trend is obvious in C_{30} alkyl keto-ols from 0 to 195.07 mcd, and a sharp increase occurs in some samples in the next 50-m interval (Table T1; Fig. F5). For C_{32} alkyl keto-ols, the pattern is similar, but these were not detected in many samples. Versteegh et al. (1997) pointed out that both compound classes are diagenetically independent, but their sources are as yet unidentified.

Paleoproductivity

From the accumulation rate of marine microalgae biomarkers, variation in marine paleoproductivity can be illustrated. All the sectional accumulation rate fluctuations of the C_{37} + C_{38} alkenones, C_{30} alkyl diols,

and C_{30} + C_{32} alkyl keto-ols are quite similar, with high values in intervals 202–245 and 0–162 mcd (Fig. F7). As discussed above, the pattern may be related to East Asian monsoon development and variation. Lipids from marine sources are almost absent from the deeper part of the core (from 250 m onward), indicating low productivity and/or severe diagenetic degradation.

F7. Accumulation rates of alkenones, diols, and keto-ols, p. 15.

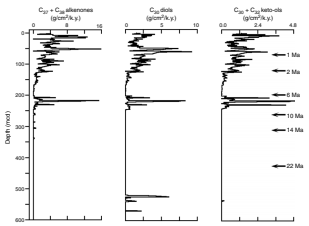

CONCLUSIONS

The lipid biomarkers in the SCS sediments from Sites 1147 and 1148 are from both terrestrial and marine sources. Long-chain *n*-alkanes, *n*-alcohols, and *n*-acids with high CPI values are mainly from higher plant leaf waxes. C_{37} and C_{38} di- and triunsaturated methyl and ethyl ketones and alkyl diols and keto-ols are of marine microalgae origin. The downhole terrigenous lipid concentrations and accumulation rates fluctuate in large ranges, with relatively higher values in intervals 0–166, 202–245, and below 495 mcd. The marine lipids are mainly found in the upper part of the hole (0–250 mcd) but are absent from the lower part of the hole. The accumulation rates of terrigenous and marine lipids indicate large inputs of allochthonous higher plant materials and blooms of autochthonous microalgae in the period of 6–8 Ma, which may be related to the development of the East Asian monsoon. After ~3.2 Ma, variations in the accumulation rates of terrigenous and marine lipids indicate the variable nature of the climate and oceanic settings, especially that of the East Asian monsoon. The pronounced late Oligocene inputs of terrigenous lipids reflect the paleoenvironment of a newly opened, narrow basin, with restricted ocean waters and the proximity of continental runoff.

ACKNOWLEDGMENTS

This research used samples and data provided by the Ocean Drilling Program (ODP). ODP is sponsored by the U.S. National Science Foundation (NSF) and participating countries under management of Joint Oceanographic Institutions (JOI), Inc. Funding for this research was provided by National Science Foundation of China (grant numbers 49425304 and 40103006) and National Key Basic Research Special Funds (grant number 200078500).

REFERENCES

Brassell, S.C., Eglinton, G., Marlowe, I.T., Pflaumann, U., and Sarnthein, M., 1986. Molecular stratigraphy: a new tool for climatic assessment. *Nature,* 320:129–133.

Briais, A., Patriat, P., and Tapponnier, P., 1993. Updated interpretation of magnetic anomalies and seafloor spreading stages in the South China Sea: implications for the Tertiary tectonics of Southeast Asia. *J. Geophys. Res.,* 98:6299–6328.

Cranwell, P.A., 1973. Chain-length distribution of *n*-alkanes from lake sediments in relation to post-glacial environmental change. *Freshwater Biol.,* 3:259–265.

de Leeuw, J.W., Rijpstra, W.I.C., and Schenck, P.A., 1981. The occurrence and identification of C_{30}, C_{31} and C_{32} alkan-1,15-diols and alkan-15-one-1-ols in Unit I and Unit II Black Sea sediments. *Geochim. Cosmochim. Acta,* 45:2281–2285.

Ding, Z.L., Sun, J.M., Yang, S.L., and Liu, T.S., 1998. Preliminary magnetostratigraphy of a thick eolian red-clay loess sequence at Lingtai, the Chinese Loess Plateau. *Geophys. Res. Lett.,* 25:1225–1228.

Eglinton, G., and Hamilton, R.J., 1967. Leaf epicuticular waxes. *Science,* 156:1322–1335.

Gagosian, R.B., Peltzer, E.T., and Merrill, J.T., 1987. Long-range transport of terrestrially derived lipids in aerosols from the south Pacific. *Nature,* 325:800–803.

Gagosian, R.B., Peltzer, E.T., and Zafiriou, O.C., 1981. Atmospheric transport of continentally derived lipids to the tropical North Pacific. *Nature,* 291:312–314.

Kolattukudy, P.E., 1976. *Chemistry and Biochemistry of Natural Waxes:* New York (Elsevier).

Marlowe, I.T., Brassell, S.C., Eglinton, G., and Green, J.C., 1984. Long-chain unsaturated ketones and esters in living algae and marine sediments. *In* Schenck, P.A., de Leeuw, J.W., and Lijmbach, G.W.M. (Eds.), *Advances in Organic Geochemistry 1983.* Org. Geochem., 6:135–141.

Pelejero, C., and Grimalt, J.O., 1997. The correlation between the U_{37}^k index and sea surface temperature in the warm boundary: the South China Sea. *Geochim. Cosmochim. Acta,* 61:4789–4797.

Poynter, J.G., Farrimond, P., Robinson, N., and Eglinton, G., 1989. Aeolian derived higher plant lipids in the marine sedimentary record: links with palaeoclimate. *In* Leinen, M., and Sarnthein, M. (Eds.), *Palaeoclimatology and Palaeometeorology: Modern and Past Patterns of Global Atmospheric Transport:* Dordrecht (Kluwer Academic Press), 435–462.

Ruddiman, W.F. (Ed.), 1997. *Tectonic Uplift and Climate Change:* New York (Plenum).

Simoneit, B.R.T., Chester, R., and Eglinton, G., 1977. Biogenic lipids in particulates from the lower atmosphere over the eastern Atlantic. *Nature,* 267:682–685.

Versteegh, G.J.M., Bosch, H.-J., and de Leeuw, J.W., 1997. Potential paleoenvironmental information of C_{24} to C_{36} mid-chain diols, keto-ols and mid-chain hydroxy fatty acids: a critical review. *Org. Geochem.,* 27:113.

Volkman, J.K., Barrett, S.M., and Blackburn, S.I., 1999. Eustigmatophyte microalgae are potential sources of C_{29} sterols, C_{22}–C_{28} *n*-alcohols and C_{28}–C_{32} *n*-alkyl diols in freshwater environments. *Org. Geochem.,* 30:307–318.

Volkman, J.K., Barrett, S.M., Blackburn, S.I., Mansour, M.P., Sikes, E.L., and Gelin, F., 1998. Microalgal biomarkers: a review of recent research developments. *Org. Geochem.,* 29:1163–1179.

Volkman, J.K., Barrett, S.M., Blackburn, S.I., and Sikes, E.L., 1995. Alkenones in *Gephyrocapsa oceanica*: implications for studies of paleoclimate. *Geochim. Cosmochim. Acta,* 59:513–520.

Volkman, J.K., Barrett, S.M., Dunstan, G.A., and Jeffrey, S.W., 1992. C_{30}–C_{32} alkyl diols and unsaturated alcohols in microalgae of the class Eustigmatophyceae. *Org. Geochem.,* 18:131–138.

Volkman, J.K., Eglinton, G., Corner, E.D.S., and Forsberg, T.E.V., 1980. Long-chain alkenes and alkenones in the marine coccolithophorid *Emiliania huxleyi*. *Phytochemistry,* 19:2619–2622.

Wang, P., Wang, L., Bian, Y., and Jian, Z., 1995. Late Quaternary paleoceanography of the South China Sea: surface circulation and carbonate cycles. *In* Tokuyama, H., Taira, A., and Kuramoto, S. (Eds.), *Asian Marine Geology.* Mar. Geol., 127:145–165.

Figure F1. A. Gas chromatogram of total extractable lipids from Sample 184-1148A-8H-2, 56–57 cm; 59.86 mbsf. Solid circles = *n*-alkanes, open circles = *n*-fatty acids, triangles = *n*-alcohols. C_{31} = C_{31} *n*-alkane; C_{28} = C_{28} *n*-fatty acid; C_{30} = C_{30} *n*-alcohol; 1 = $C_{16:1}$ fatty acid; 2 = $C_{18:1}$ fatty acid; 3 = $C_{18:2}$ fatty acid; 4 = C_{30} diol; 5 = C_{30} keto-ol; 6 = $C_{37:3}$ methyl ketone; 7 = $C_{37:2}$ methyl ketone; 8 = $C_{38:2}$ ethyl ketone. I.S. = internal standard ($C_{16}D_{31}O_2H$), TIC = total ion chromatogram. **B.** *m/z* 85 mass chromatogram showing *n*-alkanes. Numbers refer to *n*-alkane chain length. **C.** *m/z* 132 mass chromatogram showing *n*-fatty acids. Numbers refer to *n*-fatty acid chain length. **D.** *m/z* 103 mass chromatogram showing *n*-alcohols. Numbers refer to *n*-alcohol chain length.

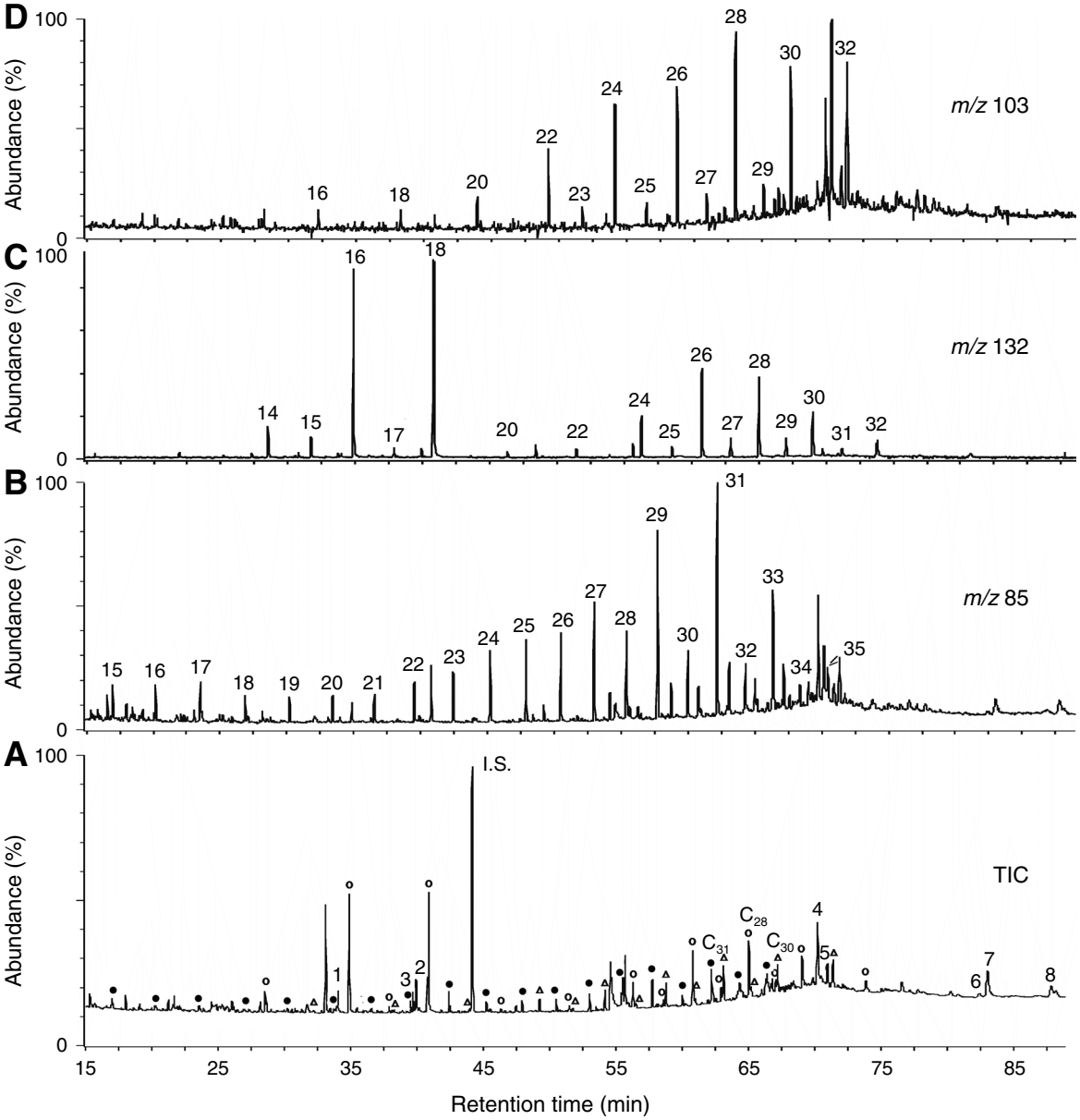

Figure F2. Site 1147 and 1148 downhole variations in carbon preference index (CPI), odd-over-even (OEP) prominence, and average chain length (ACL) of *n*-alkanes. CPI = $[(C_{25–33(odd)}/C_{24–32(even)}) + (C_{25–33(odd)}/C_{26–34(even)})]/2$; OEP = $[C_{27} + 6(C_{29} + C_{31})]/(4 \times C_{28}+4 \times C_{30})$; ACL = $(C_i \times i)/ C_i$, where i ranges from 23 to 33 for *n*-alkanes.

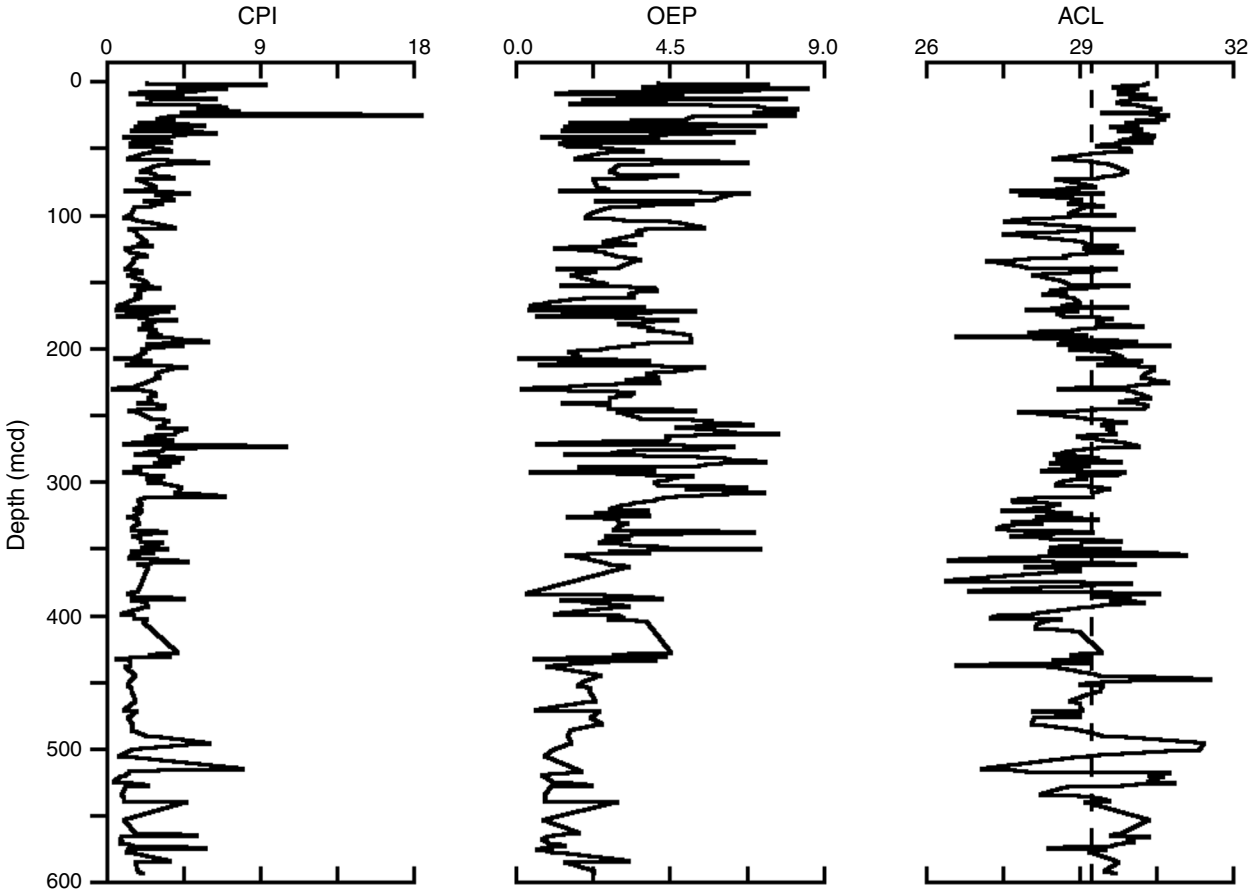

Figure F3. Variations in concentrations of C_{27} + C_{29} + C_{30} *n*-alkane, C_{26} + C_{28} + C_{30} *n*-alcohol, and C_{26} + C_{28} + C_{30} *n*-fatty acid downhole, Sites 1147 and 1148.

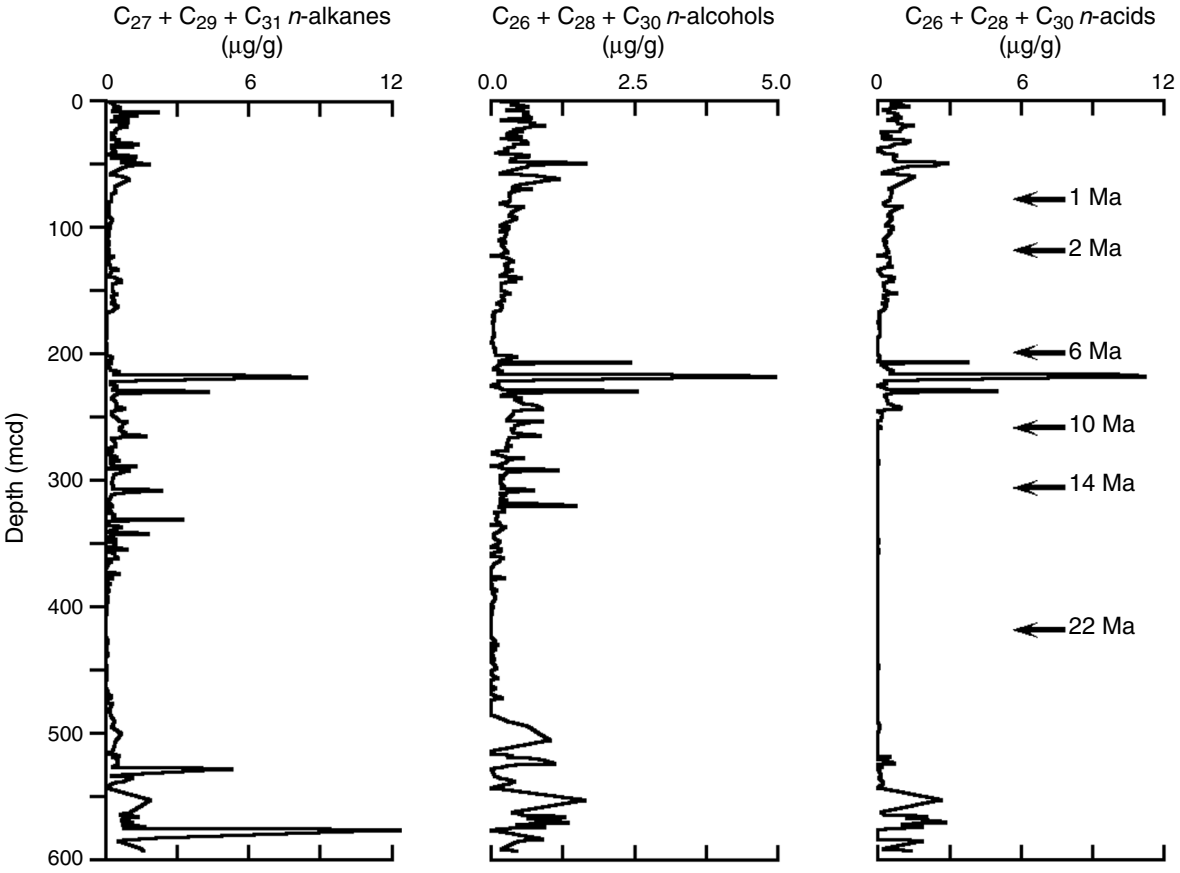

Figure F4. Variations in accumulation rates of C_{27} + C_{29} + C_{30} *n*-alkane, C_{26} + C_{28} + C_{30} *n*-alcohol, and C_{26} + C_{28} + C_{30} *n*-fatty acid downhole, Sites 1147 and 1148.

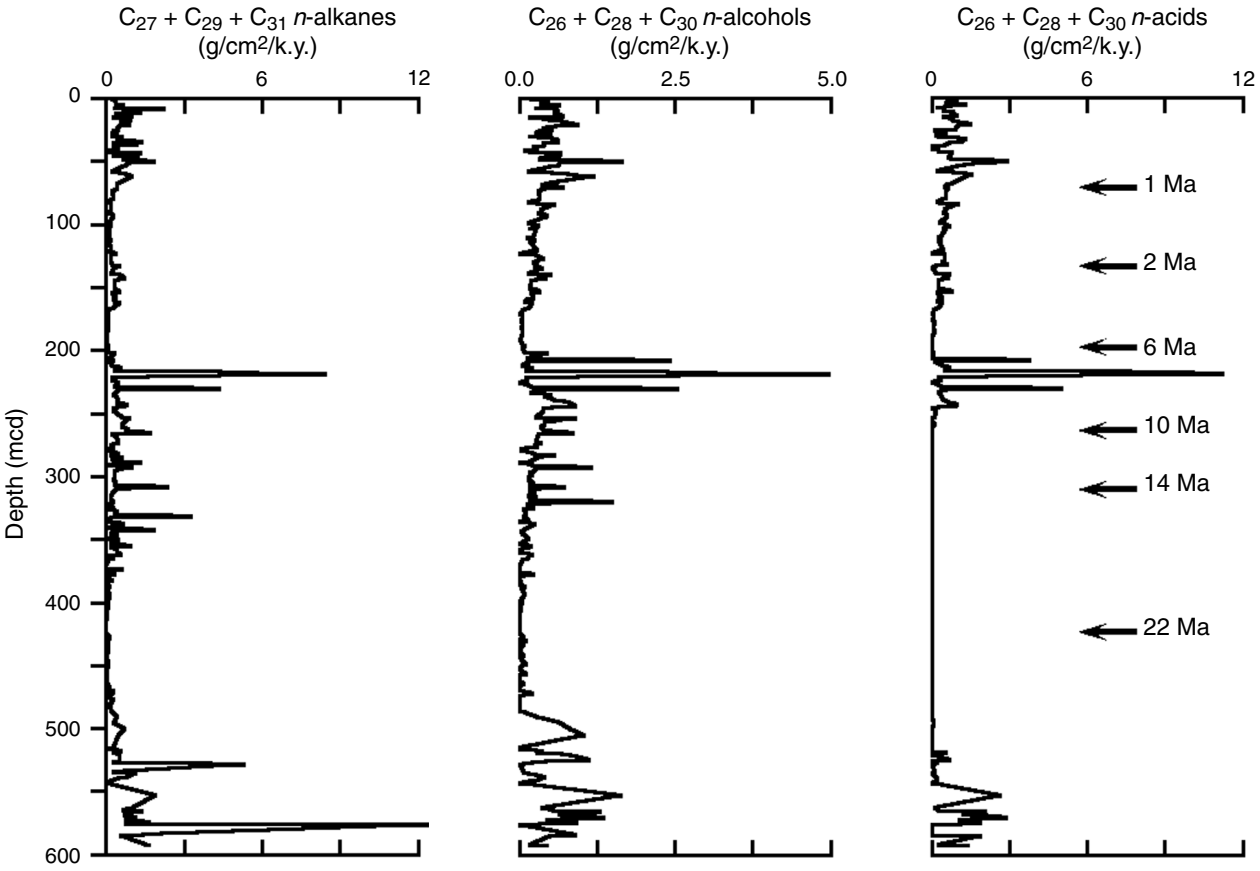

Figure F5. Variations in concentrations of C_{37} + C_{38} alkenones, C_{30} diols, and C_{30} + C_{32} keto-ols downhole, Sites 1147 and 1148.

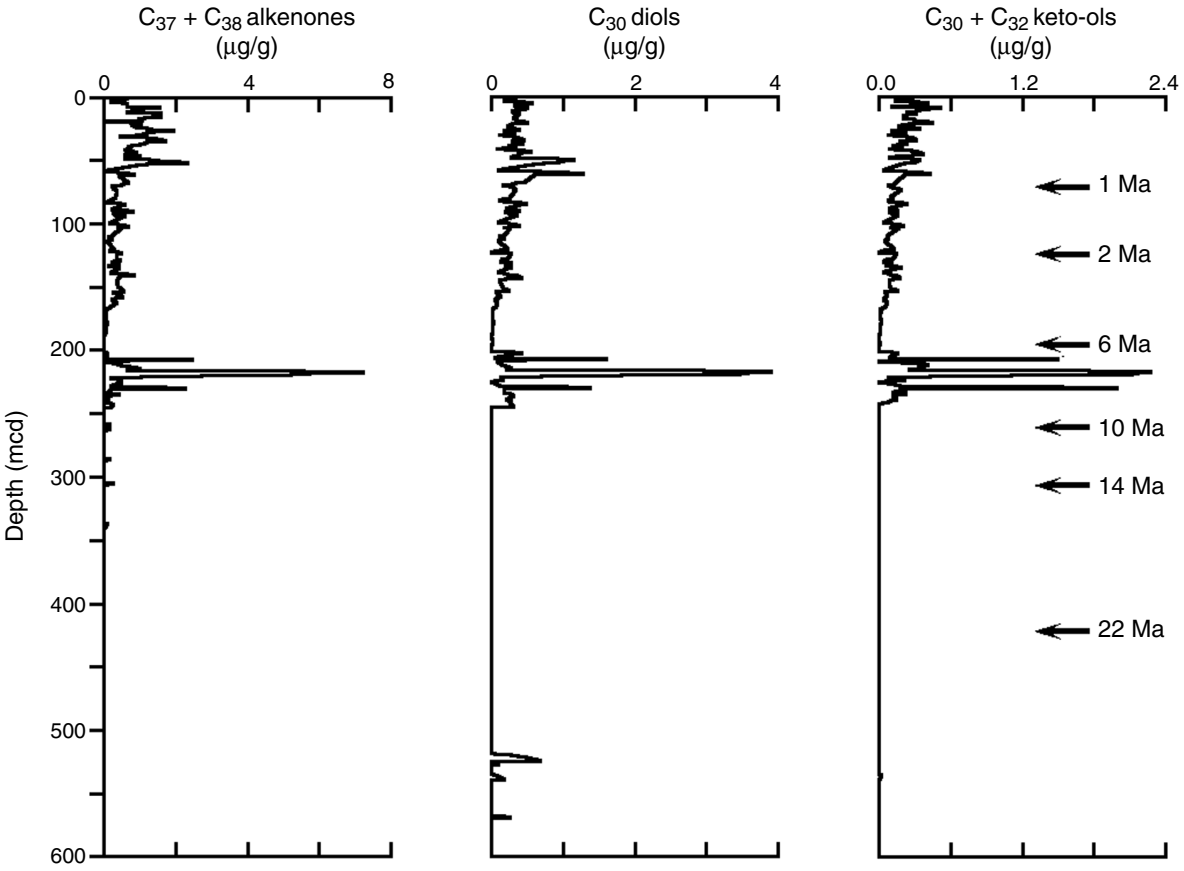

Figure F6. Variations in $U^{k'}_{37}$ values and $U^{k'}_{37}$-based sea-surface temperature (SST) within the interval of 0–200 mcd. $U^{k'}_{37} = (C_{37:2})/(C_{37:2}+C_{37:3})$. SST = $(U^{k'}_{37} - 0.092)/0.031$.

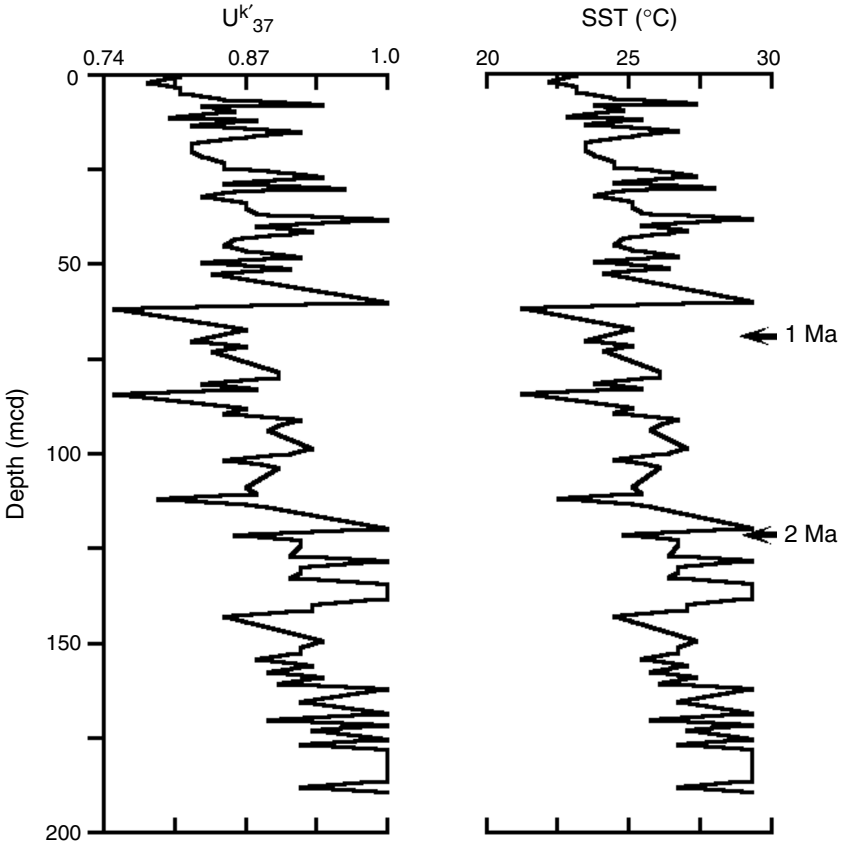

Figure F7. Variations in accumulation rates of C_{37} + C_{38} alkenones, C_{30} diols, and C_{30} + C_{32} keto-ols downhole, Sites 1147 and 1148.

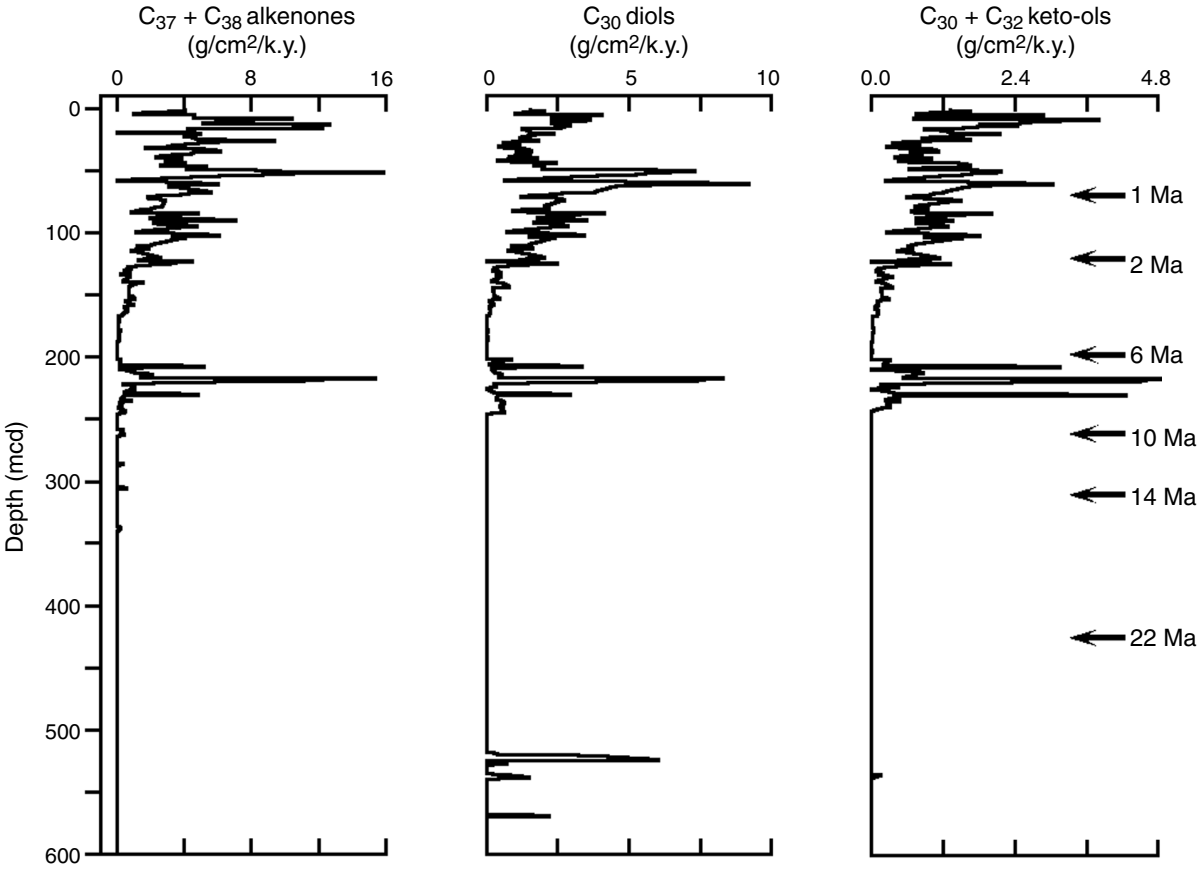

Table T1. Concentrations of marine and terrigenous lipids, Sites 1147 and 1148.

Hole, core, section	Depth (mbsf)	Depth (mcd)	Concentration (μg/g dry sediment) $C_{27} + C_{29} + C_{31}$ n-alkane	$C_{26} + C_{28} + C_{30}$ n-alcohol	$C_{26} + C_{28} + C_{30}$ n-acid	$C_{37:2}$ (me)	$C_{37:3}$ (me)	$C_{38:2}$ (et)	$C_{38:2}$ (me)	C_{30} diols	C_{30} keto-ol	C_{32} keto-ol
184-												
1147B-1H-1	0.56	0.56	0.21	0.18	0.58	0.29	0.07	0.15	0.11	0.24	0.15	0.05
1147B-1H-2	2.06	2.06	0.36	0.46	1.00	0.24	0.07	0.14	0.06	0.34	0.16	0.11
1147B-1H-3	3.56	3.56	0.35	0.34	0.57	0.09	0.02	0.04	0.02	0.18	0.08	0.05
1147B-1H-4	5.06	5.06	0.63	0.64	1.30	0.33	0.08	0.16	0.07	0.56	0.26	0.14
1147B-1H-5	6.56	6.56	0.35	0.45	0.50	0.34	0.06	0.18	0.07	0.32	0.13	0.12
1147B-1H-6	8.06	8.06	0.30	0.26	0.21	0.82	0.06	0.40	0.26	0.33	0.10	0.00
1147C-2H-4	7.66	8.26	2.20	0.56	0.49	0.63	0.13	0.33	0.00	0.49	0.30	0.22
1147C-2H-5	9.16	9.76	0.62	0.63	0.44	0.65	0.11	0.29	0.00	0.46	0.25	0.16
1147C-2H-6	10.66	11.26	1.32	0.56	0.85	0.35	0.09	0.20	0.00	0.28	0.20	0.11
1147B-2H-2	11.56	12.06	0.36	0.57	0.71	0.76	0.11	0.43	0.29	0.30	0.15	0.08
1147B-2H-3	13.06	13.56	0.96	0.70	0.98	0.73	0.16	0.37	0.07	0.37	0.18	0.13
1147B-2H-4	14.56	15.06	0.25	0.17	0.43	0.83	0.07	0.44	0.25	0.34	0.15	0.05
1147B-2H-5	16.06	16.56	0.92	0.49	0.77	0.52	0.08	0.24	0.13	0.29	0.12	0.08
1147B-2H-6	17.56	18.06	0.56	0.76	0.84	0.44	0.09	0.30	0.22	0.34	0.17	0.12
1147A-3H-2	16.96	18.71	0.67	0.67	1.03	0.00	0.00	0.00	0.00	0.34	0.17	0.13
1147A-3H-3	18.46	20.21	0.87	0.93	1.49	0.46	0.10	0.32	0.15	0.49	0.25	0.19
1147A-3H-4	19.96	21.71	0.50	0.58	1.02	0.38	0.08	0.20	0.10	0.28	0.17	0.08
1147A-3H-5	21.46	23.21	0.40	0.39	0.91	0.40	0.07	0.28	0.14	0.22	0.10	0.06
1147A-3H-6	22.96	24.71	0.43	0.53	0.94	0.62	0.11	0.39	0.22	0.32	0.20	0.14
1147C-4H-2	23.66	25.71	0.26	0.33	0.14	0.99	0.11	0.55	0.29	0.38	0.17	0.03
1147C-4H-3	25.16	27.21	0.22	0.26	0.20	0.78	0.05	0.34	0.19	0.17	0.10	0.00
1147C-4H-4	26.66	28.71	0.38	0.51	0.55	0.58	0.10	0.28	0.14	0.31	0.15	0.07
1147C-4H-5	28.16	30.21	0.22	0.17	0.18	0.43	0.02	0.23	0.13	0.11	0.05	0.02
1147B-4H-1	29.06	30.76	0.58	0.30	0.27	0.23	0.04	0.11	0.06	0.17	0.09	0.04
1147B-4H-2	30.56	32.26	0.41	0.60	1.33	0.69	0.14	0.42	0.19	0.37	0.17	0.11
1147B-4H-3	32.06	33.76	1.34	0.63	1.17	0.98	0.15	0.42	0.17	0.44	0.19	0.12
1147B-4H-4	33.56	35.26	0.26	0.39	0.69	0.55	0.08	0.35	0.20	0.28	0.12	0.05
1147B-4H-5	35.06	36.76	1.14	0.40	0.51	0.55	0.08	0.28	0.16	0.38	0.15	0.06
1147A-5H-3	34.68	36.86	0.26	0.39	0.50	0.55	0.07	0.23	0.13	0.43	0.17	0.06
1147A-5H-4	36.18	38.36	0.27	0.23	0.00	0.46	0.00	0.22	0.00	0.24	0.12	0.00
1147A-5H-5	37.68	39.86	0.42	0.28	0.01	0.38	0.05	0.22	0.08	0.34	0.13	0.06
1147A-5H-6	39.18	41.36	0.13	0.08	0.29	0.16	0.29	0.11	0.00	0.08	0.05	0.04
1147B-5H-2	40.06	41.96	0.11	0.16	0.28	0.28	0.03	0.17	0.13	0.18	0.06	0.07
1147B-5H-3	41.56	43.46	1.29	0.65	0.78	0.44	0.07	0.24	0.14	0.54	0.19	0.13
1147B-5H-4	43.06	44.96	0.25	0.64	0.70	0.48	0.09	0.00	0.00	0.37	0.20	0.16
1147B-5H-5	44.56	46.46	1.21	0.35	0.63	0.51	0.07	0.25	0.14	0.38	0.14	0.14
1148A-6H-3	42.36	48.16	0.65	0.32	0.75	0.42	0.04	0.12	0.00	0.27	0.09	0.00
1148A-6H-4	43.86	49.66	1.81	1.65	2.92	0.98	0.20	0.34	0.00	1.14	0.34	0.00
1148A-6H-5	45.36	51.16	0.85	0.64	2.43	1.29	0.13	0.56	0.33	0.94	0.30	0.00
1148A-6H-6	46.86	52.66	0.71	0.62	1.27	0.58	0.11	0.29	0.20	0.71	0.21	0.00
1148A-7H-3	51.86	57.76	0.21	0.15	0.20	0.00	0.00	0.00	0.00	0.09	0.03	0.00
1148A-7H-4	53.36	60.26	0.86	0.92	1.56	0.84	0.00	0.00	0.00	1.28	0.42	0.00
1148A-7H-5	54.86	61.76	0.98	1.19	1.37	0.24	0.08	0.07	0.00	0.59	0.21	0.00
1148A-8H-2	59.86	67.23	0.38	0.43	0.79	0.36	0.05	0.17	0.10	0.46	0.15	0.00
1148A-8H-3	61.36	68.73	0.39	0.37	0.59	0.24	0.05	0.11	0.06	0.27	0.12	0.00
1148A-8H-4	62.86	70.23	0.39	0.69	0.49	0.14	0.02	0.06	0.00	0.15	0.07	0.00
1148A-8H-5	64.36	71.73	0.41	0.40	0.62	0.12	0.02	0.05	0.04	0.30	0.11	0.00
1148A-8H-6	65.86	73.23	0.22	0.30	0.57	0.23	0.03	0.05	0.05	0.33	0.18	0.00
1148A-9H-3	70.86	78.53	0.26	0.33	0.53	0.20	0.02	0.06	0.05	0.25	0.09	0.00
1148A-9H-4	72.36	80.03	0.14	0.31	0.40	0.12	0.02	0.06	0.03	0.25	0.11	0.00
1148A-9H-5	73.86	81.53	0.08	0.14	0.23	0.09	0.01	0.02	0.01	0.10	0.08	0.00
1148A-9H-6	75.16	82.83	0.15	0.28	0.30	0.04	0.01	0.02	0.01	0.17	0.08	0.00
1148A-9H-7	76.66	84.33	0.15	0.56	1.04	0.31	0.05	0.13	0.07	0.48	0.23	0.00
1148A-10H-3	80.36	88.03	0.16	0.34	0.50	0.13	0.02	0.04	0.04	0.20	0.09	0.00
1148A-10H-4	81.86	89.53	0.11	0.36	0.54	0.44	0.04	0.18	0.13	0.39	0.15	0.00
1148A-10H-5	83.36	91.03	0.13	0.31	0.43	0.15	0.02	0.04	0.04	0.19	0.09	0.00
1148A-10H-6	84.86	92.53	0.25	0.45	0.60	0.17	0.02	0.05	0.05	0.27	0.12	0.00
1148A-10H-7	86.36	94.03	0.27	0.43	0.59	0.32	0.02	0.13	0.10	0.35	0.15	0.00
1148A-11H-3	89.86	98.58	0.09	0.15	0.30	0.08	0.01	0.03	0.02	0.09	0.03	0.00
1148A-11H-4	91.36	100.08	0.18	0.31	0.59	0.20	0.04	0.06	0.08	0.24	0.10	0.00
1148A-11H-5	92.86	101.58	0.12	0.29	0.67	0.33	0.04	0.15	0.14	0.37	0.14	0.06
1148A-11H-6	94.36	103.08	0.07	0.16	0.47	0.18	0.02	0.06	0.10	0.16	0.08	0.02
1148A-11H-7	95.13	103.85	0.13	0.26	0.55	0.19	0.03	0.09	0.12	0.26	0.13	0.03

Note: me = methyl ketone, et = ethyl ketone. Only a portion of this table appears here. The complete table is available in **ASCII**.